

Electron capture and β -decay rates for sd -shell nuclei in stellar environments relevant to high density O-Ne-Mg cores

Toshio Suzuki¹

*Department of Physics and Graduate School of Integrated Basic Sciences,
College of Humanities and Sciences, Nihon University
Sakurajosui 3-25-40, Setagaya-ku, Tokyo 156-8550, Japan
suzuki@phys.chs.nihon-u.ac.jp*

Hiroshi Toki

*Research Center for Nuclear Physics (RCNP), Osaka University,
Ibaraki, Osaka 567-0047, Japan
and*

Ken'ichi Nomoto²

*Kavli Institute for the Physics and Mathematics of the Universe (WPI),
The University of Tokyo, Kashiwa, Chiba 277-8583, Japan*

Accepted for publication in the Astrophysical Journal

ABSTRACT

Electron capture and β -decay rates for nuclear pairs in sd -shell are evaluated at high densities and high temperatures relevant to the final evolution of electron-degenerate O-Ne-Mg cores of stars with the initial masses of 8-10 M_{\odot} . Electron capture induces a rapid contraction of the electron-degenerate O-Ne-Mg core. The outcome of rapid contraction depends on the evolutionary changes in the central density and temperature, which are determined by the competing processes of contraction, cooling, and heating. The fate of the stars are determined by these competitions, whether they end up with electron-capture supernovae or Fe core-collapse supernovae. Since the competing processes are induced by electron capture and β -decay, the accurate weak rates are crucially important. The rates are obtained for pairs with $A=20, 23, 24, 25$ and 27 by shell-model calculations in sd -shell with the USDB Hamiltonian. Effects of Coulomb corrections on the rates are evaluated. The rates for pairs with $A=23$ and 25 are important for nuclear URCA processes that determine the cooling rate of O-Ne-Mg core, while those for pairs with $A=20$ and 24 are important for the core-contraction and heat generation rates in the core. We provide these nuclear rates at stellar environments in tables with fine enough meshes at various densities and temperatures for the studies of astrophysical processes sensitive to the rates. In particular, the accurate rate tables are crucially important for the final fates of not only O-Ne-Mg cores but also a wider range of stars such as C-O cores of lower mass stars.

Subject headings: nuclear reactions, nucleosynthesis, abundances - stars: AGB and post-AGB - stars: evolution - stars: supernovae

1. Introduction

The evolution and final fates of stars depend on their initial masses M_I (e.g., Nomoto et al. 2013), which is still subject to some uncertainties involved in stellar mass-loss, mixing processes and nuclear transition rates. Stars with $M_I = 0.5\text{--}8 M_\odot$ form a C-O core after He burning and become C+O white dwarfs. Stars with $M_I > 10 M_\odot$, on the other hand, form an Fe core and later explode as core-collapse supernovae. In stars with $M_I = 8\text{--}10 M_\odot$, an O-Ne-Mg core is formed after carbon burning. $8\text{--}10 M_\odot$ stars can end up in various ways, that is, as O-Ne-Mg white dwarfs without explosions, or as electron-capture supernovae or Fe core-collapse supernovae (Nomoto et al. 1988; Miyaji et al. 1980; Nomoto 1984, 1987).

The evolutionary changes in the central density and temperature of the O-Ne-Mg core are determined by the competition among the contraction, cooling and heating processes. If heating is fast enough relative to contraction, the temperature would become high enough to ignite Ne-O burning, which would result in the Fe core formation. If cooling is fast, the contraction would lead to the collapse of the O-Ne-Mg core and an electron-capture supernova. The fate of the stars with $M_I \sim 8\text{--}10 M_\odot$ is thus determined by these competitions. Since these competing processes are induced by electron capture and β -decay, the accurate weak rates are crucially important.

We study electron capture and β -decay rates in *sd*-shell nuclei at stellar environments relevant to the final evolution of electron-degenerate O-Ne-Mg cores in stars with the initial masses of $M_I = 8\text{--}10 M_\odot$. Nuclear URCA processes, especially in nuclear pairs with $A=23$ and 25 , are important for the cooling of the O-Ne-Mg cores after carbon burning (Toki et al. 2013; Jones et al. 2013). Electron capture reactions and successive gamma emissions in nuclei with $A=24$ and 20 are important for the contraction and heating of the core in later stages leading to an electron-capture supernova. The cooling and heating rates of the core as well as the core-contraction rate are determined by the weak rates for the nuclear pairs. The fate of the stars depend sensitively on the nuclear elec-

tron capture and β -decay rates.

Precise evaluations of the weak rates in stars are quite important for the evolutions of not only the stars having O-Ne-Mg cores but also lower mass stars having C-O cores (which contain primordial species of $A = 20\text{--}27$). The rates are also important for the final fates of O-Ne-Mg, C-O and hybrid C-O-Ne white dwarfs in binary systems. We thus provide electron capture and β -decay rates at stellar environments with such fine meshes as $\Delta \log_{10}(\rho Y_e) = 0.02$ (Y_e is the electron mole number and ρ is the nucleon density in units of g cm^{-3}) and $\Delta \log_{10} T = 0.05$ (T is the temperature in units of K) at various densities and temperatures, so that they can be used for the studies of astrophysical processes sensitive to the rates as well as the determination of the final fates of stars. We provide the Table for the weak rates on the web (Suzuki et al. 2015).

In sect. 2, Q -values in *sd*-shell nuclei and relations to triggering electron capture reactions are discussed. In sect. 3, formalism for electron capture and β -decay rates as well as neutrino energy-loss rate and γ -ray heating rate are given. Coulomb corrections are also taken into account. In sect. 4, the weak rates and energy loss by neutrino emissions for nuclear pairs with $A=23$, 25 and 27 , which are important for the URCA processes, are studied. Summary is given in sect. 5.

2. Q -values in *sd*-shell nuclei

The triggering of electron capture reactions is determined by Q -values of nuclear transitions and values of the chemical potential of electrons at high densities and high temperatures. The Q -values for β -decays in *sd*-shell nuclei with $A=17\text{--}31$ are shown in Fig. 1. They are taken from Wang et al. (2012).

In general, the Q -values can become small for odd- A nuclei compared to even- A nuclei as can be noticed from Fig. 1. They are particularly as small as $1.5\text{--}4.4$ MeV for the pairs with $A=23$, 25 , 27 , 29 and 31 : $^{23}\text{Ne} \rightarrow ^{23}\text{Na}$, $^{25}\text{Na} \rightarrow ^{25}\text{Mg}$, $^{27}\text{Mg} \rightarrow ^{27}\text{Al}$, $^{29}\text{Al} \rightarrow ^{29}\text{Si}$ and $^{31}\text{Si} \rightarrow ^{31}\text{P}$. The URCA processes can occur for these nuclear pairs if the transition from the ground state (g.s.) of the mother nucleus to the ground state of the daughter nucleus is not forbidden. In fact, the URCA processes for the pairs, $^{23}\text{Ne} \leftrightarrow ^{23}\text{Na}$, ^{25}Na

¹Visiting Researcher, National Astronomical Observatory of Japan, Mitaka, Tokyo 181-8588, Japan

²Hamamatsu Professor

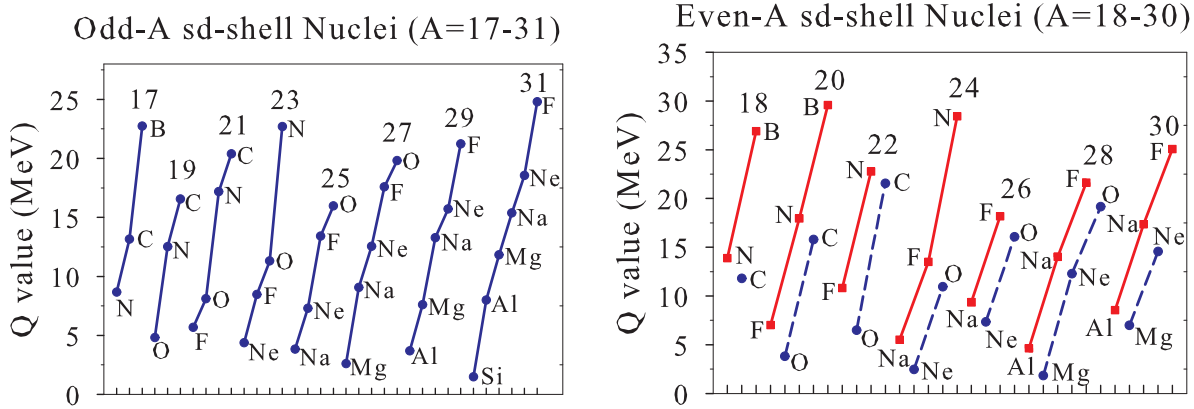


Fig. 1.— Q-values for β -decays for *sd*-shell nuclei with odd-A ($A=17-31$) and even-A ($A=18-30$). Parent nuclei with proton number Z and mass number A for β -decays, $(Z, A) \rightarrow (Z+1, A) + e^- + \bar{\nu}_e$, are denoted in the figures. Data are taken from Wang et al. (2012). For even-A case, transitions from odd-odd and even-even nuclei are shown by solid and dashed lines, respectively.

$\leftrightarrow {}^{25}\text{Mg}$, are found to be important for the cooling of the O-Ne-Mg core of stars with $8-10 M_\odot$ (Toki et al. 2013; Jones et al. 2013). As the g.s. to g.s. transition for ${}^{27}\text{Mg} \leftrightarrow {}^{27}\text{Al}$ is a forbidden transition, the URCA process does not occur for this pair (Toki et al. 2013) though the Q-value is very small; $Q=2.61$ MeV. The order of the occurrence of the URCA processes depends on the Q-value of the transition. The URCA processes for the pair ${}^{25}\text{Na}-{}^{25}\text{Mg}$ with $Q=3.83$ MeV takes place first, and it is followed by the URCA process for the pair ${}^{23}\text{Ne}-{}^{23}\text{Na}$ with $Q=4.38$ MeV.

For even-A nuclei, the β -decay Q-values are generally large for transitions from odd-odd nuclei to even-even nuclei while they are relatively small for transitions from even-even to odd-odd nuclei owing to the pairing effects. In later stages of the evolution of O-Ne-Mg core stars, electron capture reactions on even-even nuclei such as ${}^{24}\text{Mg}$ with Q-value of 5.52 MeV and ${}^{20}\text{Ne}$ with Q-value of 7.02 MeV are triggered at higher densities. They are succeeded by electron capture reactions on ${}^{24}\text{Na}$ and ${}^{20}\text{F}$, respectively. These odd-odd nuclei have small threshold energies for the electron capture reactions, 2.47 MeV for ${}^{24}\text{Na}$ and 3.81 MeV

for ${}^{20}\text{F}$. The double electron capture reactions on ${}^{24}\text{Mg}$ and ${}^{20}\text{Ne}$ become important for heating stars in later stages of star evolutions.

Here, we consider cooling of O-Ne-Mg core by URCA processes in nuclear pairs with $A=23, 25$ and 27 , and heating of stars by electron capture reactions on nuclei with $A=20$ and 24 . The cooling process occurs at $\log_{10}(\rho Y_e)=8.8-9.0$ first for ${}^{25}\text{Na}-{}^{25}\text{Mg}$ and ${}^{23}\text{Ne}-{}^{23}\text{Na}$ pairs, and then secondary one occurs at $\log_{10}(\rho Y_e)=9.3-9.8$ for other pairs with the second smallest Q-values in each mass number $A=23, 25$ and 27 (Jones 2013). The heating process occurs at $\log_{10}(\rho Y_e)=9.2-9.7$ for captures on ${}^{24}\text{Mg}$ and ${}^{20}\text{Ne}$. The successive electron captures on ${}^{24}\text{Na}$ and ${}^{20}\text{F}$ with smaller Q-values occur at $\log_{10}(\rho Y_e)=8.2$ and 8.8 . In the present work, the electron capture and β -decay rates in these *sd*-shell nuclei which concern the cooling of O-Ne-Mg core after C burning and the heating before O burning are evaluated covering the density region mentioned above, $\log_{10}(\rho Y_e)=8.0-10.0$, for relevant temperatures. The weak rates for nuclei with $A=17-28$ as well as neutrino energy-loss rates and γ -ray heating rates are obtained for densities $\log_{10}(\rho Y_e)=8.0-11.0$ in fine

steps of 0.02, and temperatures $\log_{10}T = 8.0$ -9.65 and 7.0 -8.0 in steps of 0.05 and 0.20, respectively (Suzuki et al. 2015).

3. Formulation for the weak reaction rates and Coulomb effects

The electron capture and β -decay transitions are dominantly induced by GT transitions in the present stellar conditions with densities $\log_{10}(\rho Y_e) = 8$ -10 and temperatures $\log_{10}T = 8$ -9.6. Structure of *sd*-shell nuclei are well described by a shell-model Hamiltonian, USD (Brown & Wildenthal 1983, 1987, 1988). Energy spectra, magnetic dipole (M1) and Gamow-Teller (GT) strengths with quenched spin g-factor and axial-vector coupling constant, g_A , as well as Q moments and E2 transition strengths with effective charges are systematically well reproduced with USD. The Hamiltonian has been updated by taking into account recent data. While neutron-rich O and F isotopes were too tightly bound for USD, the new versions, USDA and USDB (Brown et al. 2006; Richter et al. 2008), are free from this problem. Here, USDB is used for the evaluation of $B(GT)$ with $g_A^{\text{eff}}/g_A = 0.764$.

Electron capture rates at high densities and high temperatures are evaluated as (Fuller et al. 1980, 1982a,b, 1985; Langanke & Martinez-Pinedo 2001, 2003; Suzuki et al. 2011)

$$\begin{aligned} \lambda &= \frac{\ln 2}{6146(s)} \sum_i W_i \sum_f (B_{if}(GT) \\ &+ B_{if}(F)) \Phi^{\text{ec}}(Q_{if}) \\ \Phi^{\text{ec}}(Q_{if}) &= \int_{\omega_{\min}}^{\infty} \omega p(Q_{if} + \omega)^2 F(Z, \omega) S_e(\omega) d\omega, \\ Q_{if} &= (M_p c^2 - M_d c^2 + E_i - E_f)/m_e c^2, \\ W_i &= (2J_i + 1) e^{-E_i/kT} \\ &/ \sum_i (2J_i + 1) e^{-E_i/kT}, \end{aligned} \quad (1)$$

where ω and p are electron energy and momentum in units of $m_e c^2$ and $m_e c$, M_p and M_d are nuclear mass of parent and daughter nuclei, respectively, and E_i , E_f are excitation energies of initial and final states. J_i is the total spin of initial state. Here, $B(GT)$ and $B(F)$ are the GT and Fermi

strengths, respectively, given by

$$\begin{aligned} B_{if}(GT) &= (g_A/g_V)^2 \frac{1}{2J_i + 1} |\langle f || \sum_k \sigma^k t_+^k || i \rangle|^2 \\ B_{if}(F) &= \frac{1}{2J_i + 1} |\langle f || \sum_k t_+^k || i \rangle|^2 \end{aligned} \quad (2)$$

where $t_+ |p\rangle = |n\rangle$. In case of β -decay, t_+ is replaced by t_- ; $t_- |n\rangle = |p\rangle$. $F(Z, \omega)$ is the Fermi function, and $S_e(\omega)$ is the Fermi-Dirac distribution for electrons where the chemical potential, μ_e , is determined from the density, ρY_e , by

$$\rho Y_e = \frac{1}{\pi^2 N_A} \left(\frac{m_e c}{\hbar} \right)^3 \int_0^{\infty} (S_e - S_p) p^2 dp \quad (3)$$

where N_A is the Avogadro number and S_p is the Fermi-Dirac distribution for positrons with the chemical potential $\mu_p = -\mu_e$. It can become as large as 2 -5 (11) MeV at high densities $\log_{10}(\rho Y_e) = 8$ -9 (10). It slightly decreases as the temperature increases. The reaction rates become larger at higher densities because of the large chemical potential.

Since it is sometimes important to include GT transitions from thermally populated excited states in stellar interior, we include transitions from the excited states of the parent nucleus in addition to the ground state with the partition function W_i . When temperature becomes high and excitation energies of excited states of the parent nucleus are low, the nucleus can be thermally excited and the population of the excited states can be large. In such a case, the transitions from the excited states can give important contributions to the capture rates. In the present work, excited states with excitation energies up to $E_x = 2$ MeV are taken into account.

In case of β -decays, the integral in Eq. (1) is replaced by

$$\Phi^{\beta}(Q_{if}) = \int_1^{Q_{if}} \omega p(Q_{if} - \omega)^2 F(Z+1, \omega) (1 - S_e(\omega)) d\omega \quad (4)$$

The β -decay rates decrease as the density increases due to the blocking of the electron density in contrary to the electron capture case. There is, therefore, a density where both the electron capture and β -decay rates are balanced. When such densities depend little on temperatures, both the transitions occur simultaneously emitting both ν and $\bar{\nu}$ at

such densities, which we call "URCA densities". Here, the rates are evaluated for $8.0 < \log_{10}(\rho Y_e) < 11.0$ in fine steps of 0.02 and $8.0 < \log_{10} T < 9.65$ in steps of 0.05 and also for $7.0 < \log_{10} T < 8.0$ in steps of 0.20.

We give also formulae for the energy loss by neutrino emissions and heating by γ emissions for astrophysical applications. The neutrino energy-loss rate is given by

$$\begin{aligned}\xi &= \frac{(\ln 2)m_e c^2}{6146(s)} \sum_i W_i \sum_f (B_{if}(GT) \\ &+ B_{if}(F)) \Psi^{ec}(Q_{if})) \\ \Psi^{ec}(Q_{if}) &= \int_{\omega_{min}}^{\infty} \omega p(Q_{if} + \omega)^3 F(Z, \omega) \\ &\times S_e(\omega) d\omega\end{aligned}\quad (5)$$

for electron capture reactions, while for β -decay transitions Ψ^{ec} is replaced by

$$\Psi^\beta(Q_{if}) = \int_1^{Q_{if}} \omega p(Q_{if} - \omega)^3 F(Z+1, \omega) (1 - S_e(\omega)) d\omega. \quad (6)$$

The average energy of the emitted neutrino is obtained by the ratio

$$\langle E_\nu \rangle = \frac{\xi}{\lambda}. \quad (7)$$

The γ -ray heating rate is given by (Oda et al. 1994; Takahara et al. 1989)

$$\begin{aligned}\eta &= \frac{(\ln 2)m_e c^2}{6146(s)} \sum_i W_i \sum_f (B_{if}(GT) \\ &+ B_{if}(F)) \Gamma^{ec}(Q_{if})) \\ \Gamma^{ec}(Q_{if}) &= \int_{\omega_{min}}^{\infty} \omega p(Q_{if} + \omega)^2 E_f / m_e c^2 F(Z, \omega) \\ &\times S_e(\omega) d\omega\end{aligned}\quad (8)$$

for electron capture reactions, while for β -decay transitions Γ^{ec} is replaced by

$$\begin{aligned}\Gamma^\beta(Q_{if}) &= \int_1^{Q_{if}} \omega p(Q_{if} - \omega)^2 E_f / m_e c^2 \\ &\times F(Z+1, \omega) (1 - S_e(\omega)) d\omega.\end{aligned}\quad (9)$$

The average energy of the emitted γ is obtained by the ratio

$$\langle E_\gamma \rangle = \frac{\eta}{\lambda}. \quad (10)$$

Here, the excited states of the daughter nucleus are assumed to emit γ 's leading to its ground state (Oda et al. 1994; Takahara et al. 1989).

Next, the Coulomb corrections on the transition rates due to the electron background are studied. There are two Coulomb effects; one is the screening effects of electrons and the other is the change of threshold energy due to the change of chemical potential of the ions.

The Coulomb potential is modified due to the screening effects of relativistically degenerate electron liquid. The modification can be evaluated by using the dielectric function obtained by random phase approximation (Itoh et al. 2002). This effect is included by reducing the chemical potential of electrons by an amount equal to the modification of the Coulomb potential at the origin, $V_s(0)$ (Juodagalvis et al. 2010), where

$$\begin{aligned}V_s(r) &= Ze^2(2k_F)J(r) \\ J(r) &= \frac{1}{2k_F r} \left(1 - \frac{2}{\pi} \int \frac{\sin(2k_F q r)}{q^2 \epsilon(q, 0)} dq \right)\end{aligned}\quad (11)$$

The screening coefficient J is tabulated in Itoh et al. (2002) (see Toki et al. (2013) for more details). The electron capture and β -decay rates are slightly reduced and enhanced, respectively, by the effect.

The other effect is caused by the correction of the chemical potential of the nucleus with charge number Z , $\mu_C(Z)$, due to the interactions of the nucleus with the electron background (Slattery et al. 1982; Ichimaru 1998). The threshold energy changes by

$$\Delta Q_C = \mu_C(Z-1) - \mu_C(Z) \quad (12)$$

which gets larger for electron capture processes. The Coulomb chemical potential of a nucleus with Z in a plasma of electron number density n_e and temperature T is given by

$$\mu_C(Z) = kT f(\Gamma) \quad (13)$$

with $\Gamma = Z^{5/3} \Gamma_e$, $\Gamma_e = \frac{e^2}{kT a_e}$ and $a_e = (\frac{3}{4\pi n_e})^{1/3}$. The function f for $\Gamma > 1$ is given in Ichimaru (1998). More details are given in Toki et al. (2013). This effect results in the reduction of the electron capture rates and the enhancement of the β -decay rates.

Contribution of the second effect is larger than the first one, and thus the electron capture (β -decay) rates are reduced (enhanced). The URCA

density is shifted to a larger density region as shown in the next section.

4. Nuclear weak rates for pairs with $A=23, 25$ and 27

4.1. ^{23}Ne - ^{23}Na and ^{25}Na - ^{25}Mg pairs

The electron capture and β -decay rates for $A=23, 25$ and 27 are evaluated at densities and temperatures of stellar environments. The rates for the pair, ^{25}Na - ^{25}Mg , are shown in Fig. 2. Transitions from $5/2_{\text{g.s.}}^+$, $1/2^+$, $3/2^+$, $7/2^+$ and second $5/2^+$ states of ^{25}Mg are included for the electron capture reactions, while $5/2_{\text{g.s.}}^+$, $3/2^+$ and $1/2^+$ states of ^{25}Na are taken into account for the β -decays. Here, the Coulomb effects are not included. The electron capture rates increase as the density and the chemical potential increases. The β -decay rates, on the other hand, decrease as the density increases due to the blocking of the decays by the electrons with high chemical potential. The URCA density, where both the rates coincide, is found at $\log_{10}(\rho Y_e) = 8.77$. Dependence of the density on the temperature is quite small; $\Delta \log_{10} \rho Y_e < 0.01$ for $\log_{10} T = 8-9.2$. The URCA density is also found at $\log_{10}(\rho Y_e) = 8.92$ for the pair with $A=23$, ^{23}Ne - ^{23}Na . The temperature dependence is also as small as $\Delta \log_{10} \rho Y_e \approx 0.01$ for $\log_{10} T = 8-9.2$. It is important to evaluate the rates with fine meshes to obtain the clear URCA densities. Detailed discussion is given in Toki et al. (2013). In case of the pair with $A=27$, ^{27}Mg - ^{27}Al , where the GT transition from the initial ground state to the final ground state does not occur because of spin difference larger than 1, it is difficult to assign an URCA density due to the Q-value mismatch in the two transitions. The densities where e-capture and β -decay rates coincide depend much on the temperature for the $A=27$ case.

Here, we comment on the choice of the steps of the mesh in $\log_{10}(\rho Y_e)$ and $\log_{10} T$. Fine steps of 0.02 and 0.05 are adopted for both $\log_{10}(\rho Y_e)$ and $\log_{10} T$, respectively, as it is not easy to obtain accurate rate values from the interpolation procedure among quantities which differ by many orders of magnitude. For example, from the rates at $\log_{10}(\rho Y_e) = 7, 8, 9, 10$ and 11 only for a fixed temperature, it is not possible to get an accurate rate by interpolation procedures. The error in the

rate can be larger than a factor of 10.

It is true that a procedure using effective $\log ft$ values proposed by Fuller et al. (1985) works well for certain cases. The procedure is based on the fact that the change of the rates by orders of magnitudes comes mainly from the phase space factor, and the remaining part including the nuclear transition probability does not change drastically. As the phase space factor for the transition between ground states are taken in the procedure, the effective $\log ft$ method is valid for the cases where GT transitions between the ground states are dominant. In case that the g.s. to g.s. transitions are forbidden or transitions from excited states give essential contributions, the method becomes invalid when it is applied to the interpolation with sparse grid of densities at $\log_{10}(\rho Y_e) = 7, 8, 9, 10$ and 11 . The pairs ^{27}Al - ^{27}Mg and ^{20}F - ^{20}Ne are such examples.

In a density interval of $\Delta \log_{10}(\rho Y_e) = 0.02$ or in a temperature interval of $\Delta \log_{10} T = 0.05$, the rate ($\log_{10}(\text{rate})$) can change by 3-4 orders of magnitude (by 3-4) at most (see Fig. 2). For this order of the change in $\log_{10}(\text{rate})$ in the relevant intervals, the interpolation can be safely done with an accuracy of $\Delta \log_{10}(\text{rate}) = 0.001-0.002$. The steps of the meshes chosen here are sufficient for obtaining the rates with further finer meshes by the interpolation procedures.

Next, we compare the present results obtained with USDB with those of Oda et al. (1994). In Oda et al. (1994), USD interaction was used and experimental energies and GT transition rates available were also taken into account (Brown & Wildenthal 1985). Calculated GT strengths as well as their cumulative sums for USDB and USD are shown in Fig. 3 for the transitions $^{25}\text{Mg} \rightarrow ^{25}\text{Na}$ and $^{23}\text{Na} \rightarrow ^{23}\text{Ne}$. Experimental transition strengths to the ground states of the daughter nuclei are also shown. In both ^{25}Mg and ^{23}Na , the GT strength is more spread for USDB compared with USD and larger strength remains more in the higher excitation energy (E_x) region for USDB. The GT strengths differ little at low excitation energy region $E_x < 3$ MeV for ^{25}Mg , while for ^{23}Na their difference in the magnitude is noticed at low E_x region below 3 MeV. Calculated $B(GT)$ values for the transition to the ground state of ^{25}Na for both USDB and USD are consistent with the experimental value. The

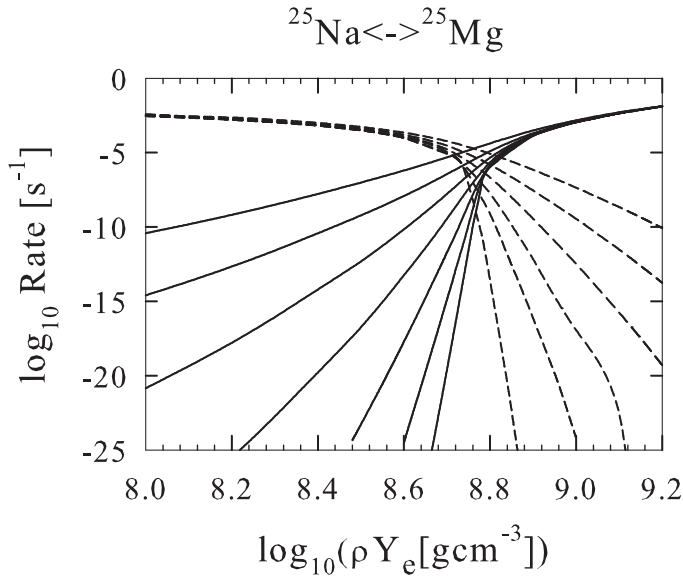


Fig. 2.— β -decay and electron capture rates for the $A=25$ URCA nuclear pairs, $^{25}\text{Na} \leftrightarrow ^{25}\text{Mg}$, for various temperatures, $\log_{10}T = 8.0-9.2$ in steps of 0.2, as functions of density $\log_{10}(\rho Y_e)$. β -decay rates (dashed curves) decrease with density while electron capture rates (solid curves) increase with density.

latter is only a bit larger than the values of USDB (USD) by 15% (19%). Transition rates are little affected by the use of experimental data for the pair $^{25}\text{Mg} \leftrightarrow ^{25}\text{Na}$. The present calculated rates with USDB are close to the rates given in Oda et al. (1994).

In case of ^{23}Na , calculated $B(GT)$ values for the transition to the ground state of ^{23}Ne are smaller than the experimental value by factors 2.67 and 1.96 for USDB and USD, respectively. Use of experimental $B(GT)$ values enhance the transition rates for the pair $^{23}\text{Na} \leftrightarrow ^{23}\text{Ne}$ about by a factor of 2.5. When experimental data are taken into account, the rates for USDB become very close to those by Oda et al. (1994) as shown in Table 1. Effects of the use of the experimental $B(GT)$ values are important. Though the rms deviation of calculated GT matrix elements from experimental ones is as small as 0.114 for USDB with the quenching factor (Richter et al. 2008), experimental $B(GT)$ values as well as experimental excitation energies are taken into account here (Suzuki et al. 2015) when they are available (NNDC ; Tilley et al. 1998; Endt 1998).

Effects of the Coulomb corrections on the tran-

sition rates are studied for the nuclear pairs, $^{23}\text{Ne} \leftrightarrow ^{23}\text{Na}$ and $^{25}\text{Na} \leftrightarrow ^{25}\text{Mg}$. The calculated rates for a temperature $\log_{10}T = 8.7$ are shown in Fig. 4 for the pairs with and without the Coulomb effects. The URCA density is shifted toward a higher density region by $\Delta \log_{10}(\rho Y_e) = 0.04$. Though the change of the URCA density is rather modest, it can affect the fate of the stars with mass around $9M_{\odot}$.

Now we discuss energy loss by neutrino emissions as well as heating by γ emissions during the electron capture and β -decay processes. Averaged energy of emitted neutrinos defined by Eq. (7), $\langle E_{\nu} \rangle$, and averaged energy production

$$\langle E_{\text{prod}} \rangle = \mu_e - Q_{\text{nucl}} - \langle E_{\nu} \rangle \quad (14)$$

with $Q_{\text{nucl}} = M_d c^2 - M_p c^2$, which is the energy difference between the g.s.'s of daughter and parent nuclei, for electron capture processes and

$$\langle E_{\text{prod}} \rangle = Q_{\text{nucl}} - \mu_e - \langle E_{\nu} \rangle \quad (15)$$

for β -decay processes are shown in Figs. 5 and 6 for $^{25}\text{Na} \leftrightarrow ^{25}\text{Mg}$ and $^{23}\text{Ne} \leftrightarrow ^{23}\text{Na}$ pairs, respectively. The energy generation in the star is determined

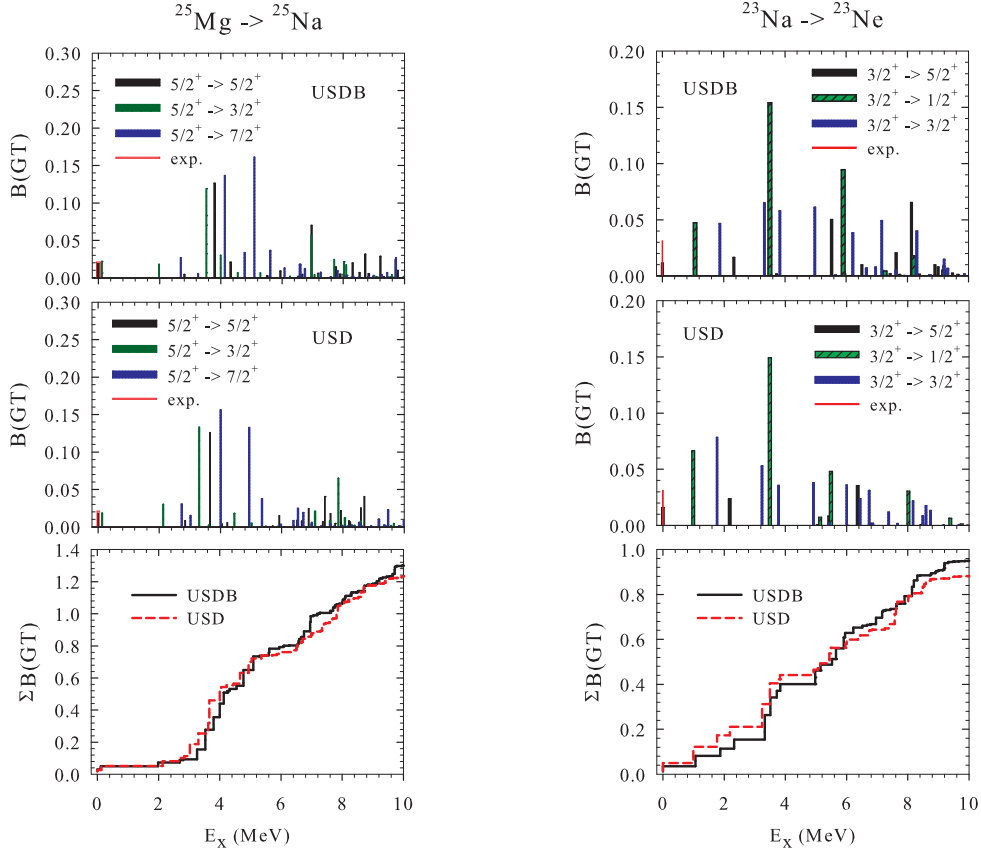


Fig. 3.— GT strengths and their cumulative sums for ^{25}Mg and ^{23}Na obtained with USDB and USD as well as the experimental values for the transition to the ground states of the daughter nuclei.

by (Martinez-Pinedo et al. 2014)

$$kT \frac{ds}{dt} = \frac{dY_e}{dt} < E_{\text{prod}} > \quad (16)$$

where s is the entropy per nucleon. The condition that the time scale for thermodynamical equilibrium is shorter than the time scale for the weak interaction is assumed to be satisfied.

Averaged neutrino energies, $\langle E_\nu \rangle$, and averaged energy productions, $\langle E_{\text{prod}} \rangle$, for electron capture reactions on ^{25}Mg and ^{23}Na and β -decay transitions from ^{25}Na and ^{23}Ne are shown in Figs. 5 and 6. The value of $\langle E_\nu \rangle$ is almost determined by the values of the electron chemical potential and the threshold energy Q_{nucl} . In case of electron capture reactions on ^{25}Mg and ^{23}Na , the neutrino energy-loss increases above the URCA densities and the increase of the averaged energy produc-

tion starts to be suppressed just at the densities, where the energy production becomes positive. In case of β -decay transitions from ^{25}Na and ^{23}Ne , the energy production is suppressed due to neutrino emissions below the URCA densities, while when it becomes negative at the URCA densities the negative energy production, that is, the energy loss begins to increase monotonically as the density increases. In both cases of electron capture and β -decay processes, the energy production is suppressed by neutrino emissions when it becomes positive. In case with the Coulomb effects, Q_{nucl} is replaced by $Q_{\text{nucl}} + \Delta Q_C$ and μ_e by $\mu_e - V_s(0)$. As ΔQ_C is positive and its magnitude is larger than $|V_s(0)|$, $\langle E_{\text{prod}} \rangle$ gets reduced (enhanced) for the electron capture (β -decay) case. This change of $\langle E_{\text{prod}} \rangle$, however, is suppressed above (below) the URCA densities for the electron capture

TABLE 1

TRANSITION RATES FOR ^{23}Na - ^{23}Ne PAIR. USDB* DENOTES THAT AVAILABLE EXPERIMENTAL DATA ARE TAKEN INTO ACCOUNT. VALUES FOR USD* ARE TAKEN FROM ODA ET AL. (1994).

ρY_e	$T/10^9$	electron-capture rates				β -decay rates			
		USDB	USDB*	USD	USD*	USDB	USDB*	USD	USD*
10^8	0.1	-2.418	-2.048	-2.284	-2.064
	0.4	-37.243	-36.899	-37.108	-36.913	-2.417	-2.048	-2.284	-2.063
	1.0	-17.640	-17.261	-17.505	-17.278	-2.414	-2.044	-2.280	-2.060
	2.0	-10.644	-10.256	-10.508	-10.270	-2.395	-2.028	-2.257	-2.042
10^9	0.1	-4.762	-4.333	-4.626	-4.352	-24.294	-23.866	-24.158	-23.185
	0.4	-4.710	-4.282	-4.574	-4.299	-10.700	-10.271	-10.564	-10.290
	1.0	-4.461	-4.046	-4.324	-4.064	-7.265	-6.854	-7.102	-6.863
	2.0	-3.965	-3.580	-3.824	-3.597	-5.275	-5.015	-5.073	-4.983

(β -decay) case since $\langle E_\nu \rangle$ with the screening effects is smaller (larger) than that without the effects. These features are seen in Figs. 5 and 6. We will show calculated results with the Coulomb effects hereafter.

4.2. ^{23}F - ^{23}Ne , ^{25}Ne - ^{25}Na and ^{27}Na - ^{27}Mg pairs

After the cooling of the O-Ne-Mg core of the stars occur by nuclear URCA processes for pairs with $A = 25$ and 23 , successive electron capture reactions are expected to be triggered at higher densities corresponding to the Q -values. Electron capture reactions on ^{24}Mg with $Q = 5.52$ MeV is considered to be important in later stages of the star evolutions leading to electron-capture supernova explosions.

The product of electron capture and β -decay rates for various nuclear pairs are shown in Fig. 7. The peak position for each pair is determined by the Q -value of each transition. The URCA densities for the pairs, ^{24}Na - ^{24}Mg , ^{25}Ne - ^{25}Na , ^{23}F - ^{23}Ne and ^{27}Na - ^{27}Mg , increase in this order. For the pair ^{20}F - ^{20}Ne , GT transition can not occur between the g.s.'s as the g.s. of ^{20}F is 2^+ while that of ^{20}Ne is 0^+ . In this case, the contributions from the forbidden transitions between the g.s.'s are taken into account (Martinez-Pinedo et al. 2014). The peak at lower density at $\log_{10}(\rho Y_e) \approx 9.2$ corresponds to the transition between ^{20}Ne (2^+) and ^{20}F (2^+) while the peak at higher density

at $\log_{10}(\rho Y_e) \approx 9.7$ corresponds to the transition between ^{20}Ne (0^+) and ^{20}F (1^+). The peak at $\log_{10}(\rho Y_e) \approx 9.5$ corresponds to the forbidden transition between the ground states. For ^{24}Mg and ^{20}Ne , the heating of stars occur by double electron capture reactions due to the pairing effects, that is, by successive electron capture reactions on ^{24}Na and ^{20}F following the capture reactions on ^{24}Mg and ^{20}Ne , respectively.

Averaged neutrino energies, $\langle E_\nu \rangle$, and averaged energy productions, $\langle E_{\text{prod}} \rangle$, for electron capture reactions on ^{25}Na and β -decay transitions from ^{25}Ne are shown in Fig. 8. Here, transitions from $5/2^+_{\text{g.s.}}$, $3/2^+$ and $1/2^+$ states of ^{25}Na are included for the electron capture reactions, while those from $1/2^+_{\text{g.s.}}$, $5/2^+$ and $3/2^+$ states of ^{25}Ne are included for the β -decays.

For the ^{25}Ne - ^{25}Na , ^{23}F - ^{23}Ne and ^{27}Mg - ^{27}Na pairs, general features of the neutrino energy-loss and energy production are similar to the cases of ^{25}Na - ^{25}Mg and ^{23}Ne - ^{23}Na pairs. Averaged energy produced is suppressed by neutrino emissions above (below) the URCA densities for electron capture (β -decay) processes.

When the production yield of ^{24}Mg from ^{12}C + ^{12}C reactions is small and the contribution of electron capture reactions on ^{24}Mg to the evolution of stars is suppressed, the URCA processes for the present pairs can be important. In a recent model of O-Ne-Mg white dwarfs, these secondary coolings induced by the pairs give important ef-

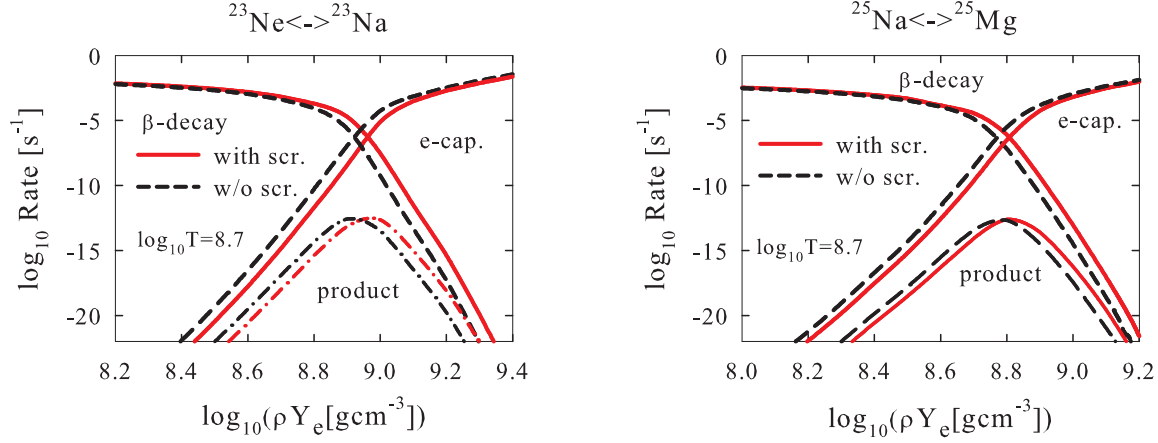


Fig. 4.— Coulomb screening effects on electron capture and β -decay rates for the $A=23$ URCA nuclear pair, $^{23}\text{Ne} \leftrightarrow ^{23}\text{Na}$, and $A=25$ URCA nuclear pair, $^{25}\text{Na} \leftrightarrow ^{25}\text{Mg}$. Solid and dashed curves are obtained with and without the screening effects, respectively, at $\log_{10}T = 8.7$. The product of the electron capture and the β -decay rates is also shown.

fects on the evolution of the stars (Jones 2013; Denissenkov et al. 2014).

We briefly comment on electron capture and β -decay rates for nuclear pairs with $A=20$ and 24 , $^{20}\text{O} \leftrightarrow ^{20}\text{F}$, $^{20}\text{F} \leftrightarrow ^{20}\text{Ne}$, and $^{24}\text{Ne} \leftrightarrow ^{24}\text{Na}$, $^{24}\text{Na} \leftrightarrow ^{24}\text{Mg}$. These weak rates are important for late stages of the evolution of stars with $8\text{--}10 M_{\odot}$. Electron capture reactions on ^{24}Mg and ^{20}Ne are important processes toward electron-capture supernova explosions or Fe core-collapse supernova explosions after contraction of the electron-degenerate O-Ne-Mg cores.

The weak rates for these nuclei are examined in detail in Martinez-Pinedo et al. (2014) by taking into account the forbidden transitions between ^{20}Ne ($0_{\text{g.s.}}^+$) and ^{20}F ($2_{\text{g.s.}}^+$). The transitions are found to give non-negligible contributions at $\log_{10}T < 9.0$ in a density region; $9.3 < \log_{10}(\rho Y_e) < 9.6$. Calculated rates with the inclusion of the forbidden transitions are also tabulated in Suzuki et al. (2015). The rates were also examined in Takahara et al. (1989) with the use of USD and available experimental data, but the effects of the forbidden transitions were not taken into account. The GT strength for $0_{\text{g.s.}}^+ \rightarrow 1^+$ (1.057 MeV) obtained from recent experimental (p, n) data on ^{20}Ne and used in Martinez-Pinedo et al. (2014) were not also taken into account as the data were not available in

1989. The GT strength, enhanced in the (p, n) data compared with the USD value, enhances the electron capture rates on ^{20}Ne at $\log_{10}(\rho Y_e) > 9.6$ about by 60-70%.

As the Q value for the $^{24}\text{Ne} \leftrightarrow ^{24}\text{Na}$ pair is as small as $Q = 2.47$ MeV due to the pairing effects, electron capture reactions on ^{24}Na occur successively after the electron capture process on ^{24}Mg , and contribute to heating the stars at later stages of evolutions leading to the electron-capture supernova or Fe-core formation. The situation is the same as in the successive electron capture reaction on ^{20}F after the capture reaction on ^{20}Ne .

5. Summary

We have studied electron capture and β -decay processes relevant to stars with O-Ne-Mg cores. Nuclear weak rates for sd -shell nuclei in stellar environments are evaluated by shell-model calculations with the use of the USDB Hamiltonian. The weak rates for nuclear pairs with $A=23$ and 25 , $^{23}\text{Ne} \leftrightarrow ^{23}\text{Na}$ and $^{25}\text{Na} \leftrightarrow ^{25}\text{Mg}$, are important for nuclear URCA processes and cooling of the O-Ne-Mg core of the stars. Evaluations of the rates with fine meshes of density and temperature are required to get clear URCA densities (Toki et al. 2013). Coulomb effects due to electron screening and change of chemical potential of ions with

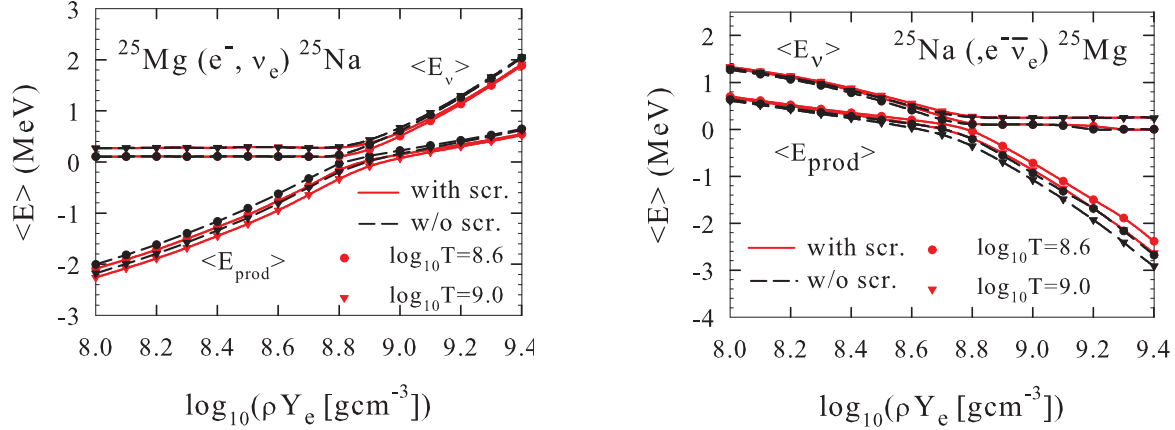


Fig. 5.— Averaged neutrino energy, $\langle E_\nu \rangle$, and averaged energy production, $\langle E_{\text{prod}} \rangle$, in electron capture reactions on ^{25}Mg and β -decay transitions from ^{25}Na for temperatures $\log_{10} T = 8.6$ and 9.0 as functions of density $\log_{10}(\rho Y_e)$. Cases with and without the screening effects are denoted by solid and dashed curves, respectively.

electron background are evaluated for the weak transitions. The effects lead to enhancements of the threshold energy for electron capture reactions and Q-value for the β -decays. The Coulomb corrections shift the URCA densities toward a higher density region.

Triggering of electron capture reactions is determined by the threshold energy of the transitions and chemical potential of electrons at high densities and temperatures. The capture reactions occur in order from pairs with smaller Q-values. After the first cooling of stars by the URCA processes for the pairs, ^{25}Na - ^{25}Mg and ^{23}Ne - ^{23}Na , electron capture reactions on ^{24}Mg , ^{25}Na , ^{23}Ne and ^{27}Mg occur successively in this order as the density increases and the chemical potential of electron is increased and reach the corresponding threshold energy. Secondary cooling of stars by the URCA processes in these nuclei can be important at higher densities (Jones 2013).

The neutrino energy-loss rate and γ -ray heating rate are also evaluated by shell-model calculations. The averaged neutrino energies and av-

eraged energy production in the electron capture and β -decay processes are obtained for the pairs, and the effects of energy loss by neutrino emissions are examined. Energy production is found to be suppressed by neutrino emissions above (below) the URCA densities for electron capture (β -decay) processes.

Usually, the heating process by electron capture reactions on ^{24}Mg and ^{20}Ne occur after the cooling by the URCA processes in the ^{25}Na - ^{25}Mg and ^{23}Ne - ^{23}Na pairs. If this heating was not enough by some reason, for example, by a lack of enough amount of ^{24}Mg , the secondary cooling by URCA processes in ^{25}Ne - ^{25}Na , ^{23}F - ^{23}Ne and ^{27}Na - ^{27}Mg pairs might have important roles in the evolution of stars (Jones 2013; Denissenkov et al. 2014).

Accurate evaluations of the nuclear weak rates at stellar environments are quite important for the studies of evolution of stars with 8-10 M_\odot . The weak rates determine the final fates of O-Ne-Mg cores and related white dwarfs but also a wider range of lower mass stars with C-O cores, which contain primordial species of $A = 20$ -27. For future

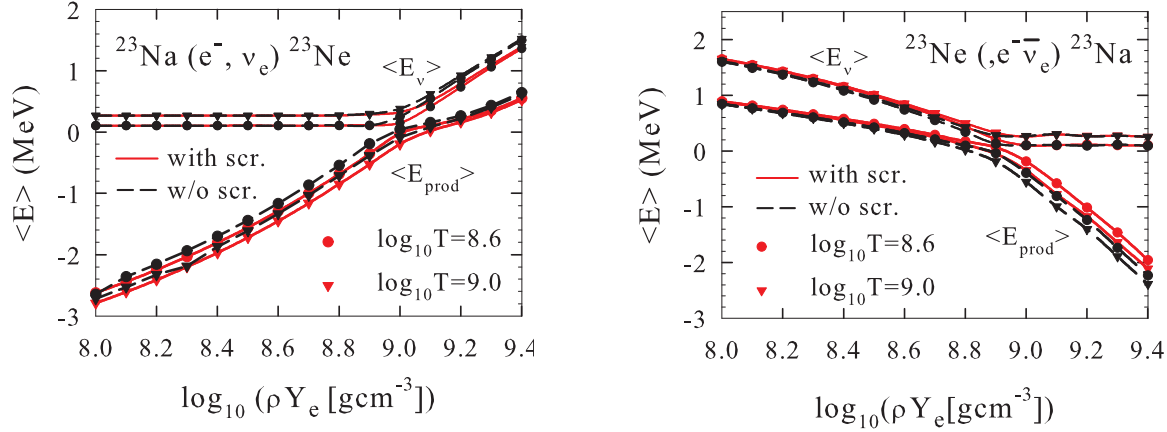


Fig. 6.— The same as in Fig. 4 for electron capture reactions on ^{23}Na and β -decay transitions from ^{23}Ne .

advances for the studies, the electron capture and β -decay rates, neutrino energy-loss rates and γ -ray heating rates for sd -shell nuclei with $A=17$ -28 have been evaluated with the Coulomb effects and tabulated for densities $\log_{10}(\rho Y_e) = 8.0$ -11.0 and temperatures $\log_{10} T = 7.0$ -9.65 with fine meshes (Suzuki et al. 2015). The weak-rate data for the pairs with $A = 23$ and 25 have been applied to study the cooling of O-Ne-Mg cores by the nuclear URCA processes and evolution of stars with 8–10 M_{\odot} (Jones et al. 2013). Stars with $M_{\text{I}} = 8.8 M_{\odot}$ are found to end up with electron-capture supernovae due to the nuclear URCA processes, while stars with $M_{\text{I}} = 9.5 M_{\odot}$ are found to evolve to Fe core-collapse supernovae. Evolution of hybrid C-O-Ne white dwarfs as progenitors of type Ia supernovae has been also studied with the nuclear URCA processes (Denissenkov et al. 2014). The hybrid progenitor models might explain the observed diversity of Type Ia supernovae.

We notice from Fig. 1 that the β -decay Q value for $^{31}\text{Si} \rightarrow ^{31}\text{P}$ is as small as 1.49 MeV. The β -decay Q value for $^{29}\text{Al} \rightarrow ^{29}\text{Si}$ is also as small as 3.69 MeV. Electron capture processes on ^{31}P and ^{29}Si could have some important roles on the cooling and neutronization of the core in later O

burning and Si burning stages in more massive stars.

The authors would like to thank Sam Jones for useful communications on evolutions of stars with O-Ne-Mg core. This work has been supported in part by Grants-in-Aid for Scientific Research (S)23224008, (S)21540267, (C)22540290, (C)26400222, and (C)15k05090, and the World Premier International Research Center Initiative of the MEXT of Japan.

REFERENCES

- Brown, B. A., & Richter, W. A. 2006, Phys. Rev. C, 74, 034315
- Brown, B. A., & Wildenthal, B. H. 1983, Phys. Rev. C, 28, 2397
- Brown, B. A., & Wildenthal, B. H. 1985, Atomic Data and Nuclear Data Tables, 33, 347
- Brown, B. A., & Wildenthal, B. H. 1987, Nucl. Phys. A, 474, 290
- Brown, B. A., & Wildenthal, B. H. 1988, Ann. Rev. Nucl. Part. Sci., 38, 29

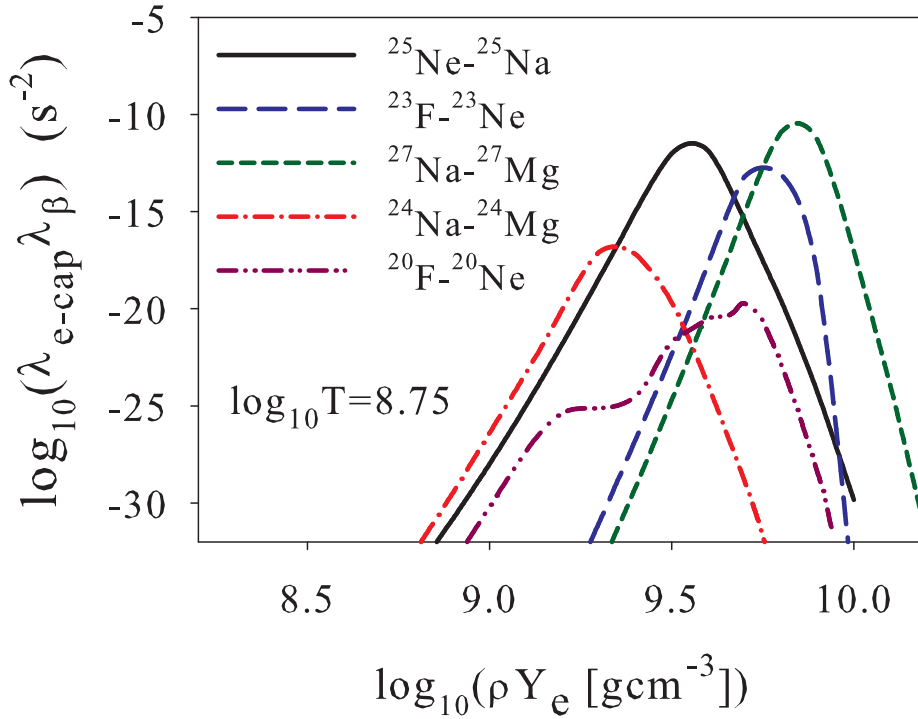


Fig. 7.— The product of electron capture and β -decay rates are shown for the nuclear pairs, ^{25}Ne - ^{25}Na , ^{23}F - ^{23}Ne , ^{27}Na - ^{27}Mg , ^{24}Na - ^{24}Mg and ^{20}F - ^{20}Ne for a temperature $\log_{10}T = 8.75$ as functions of density $\log_{10}(\rho Y_e)$.

- Denissenkov, P. A., Truran, J. W., Herwig, F., Jones, S., Paxton, B., Nomoto, K., Suzuki, T. & Toki, H 2015, MNRAS, 447, 2696
- Endt, P. M. 1998, Nucl. Phys. A, 633, 1
- Fuller, G. M., Fowler, W. A., & Newton, M. J. 1980, ApJS, 42, 447
- Fuller, G. M., Fowler, W. A., & Newton, M. J. 1980, ApJS, 1982, **48**, 279
- Fuller, G. M., Fowler, W. A., & Newton, M. J. 1982, ApJ, 252, 715
- Fuller, G. M., Fowler, W. A., & Newton, M. J. 1985, ApJ, 293, 1
- Ichimaru, S 1993, Rev. Mod. Phys., 65, 255
- Itoh, N., Tomizawa, N., Tamamura, M., & Wanajo, S 2002, ApJ, 579, 380
- Jones, S., Hirschi, R., Nomoto, K., Fiescher, T., Timmes, F. X., Herwig, F., Paxton, B., Toki, H., Suzuki, T., Martinez-Pinedo, G., Lam, Y. H., & Bertoli, M. 2013, ApJ, 772, 150
- Jones, S. 2013, PhD Thesis, Department of Physics, University of Keele
- Juodagalvis, A., Langanke, K., Hix, W. R., Martinez-Pinedo, G., & Sampaio, J. M. 2010, Nucl. Phys. A, 848, 454
- Langanke, K., & Martinez-Pinedo, G 2001, At. Data Nucl. Data Tables, 79, 1
- Langanke, K., & Martinez-Pinedo, G 2003, Rev. Mod. Phys., 75, 819
- Martinez-Pinedo, G., Lam, Y. H., Langanke, K., Zegers, R. G., & Sullivan, C. 2014, Phys. Rev. C, 89, 045806
- Miyaji, S., Nomoto, K., Yokoi, K., & Sugimoto, D. 1980, Pub. Astron. Soc. Jpn. 32, 303

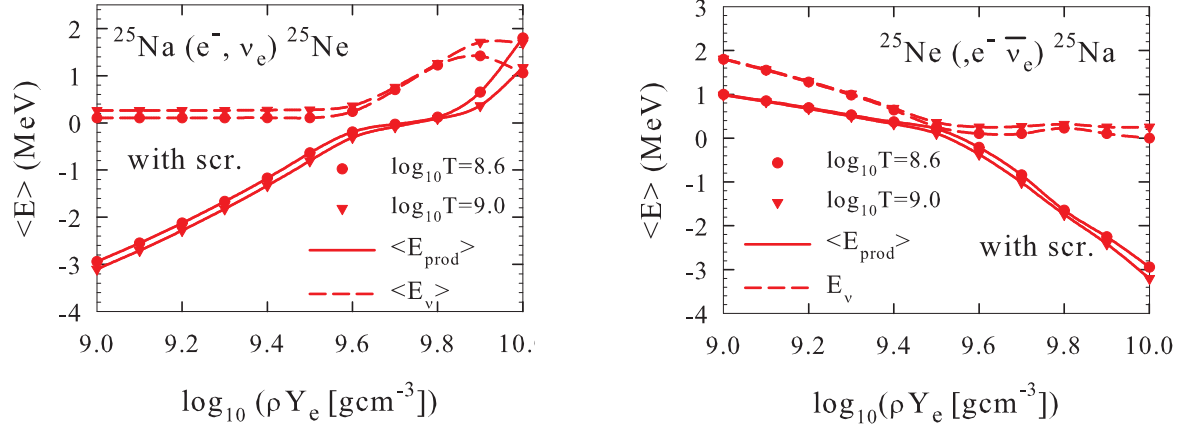


Fig. 8.— The same as in Fig. 4 for electron capture reactions on ^{25}Na and β -decay transitions from ^{25}Ne . The Coulomb corrections (screening effects) are included. Evaluated values for $\langle E_{\text{prod}} \rangle$ and $\langle E_{\nu} \rangle$ are denoted by solid and dashed curves, respectively.

National Nuclear Data Center on-line retrieval system, <http://www.nndc.bnl.gov>

Nomoto, K. 1984, *ApJ*, 277, 791

Nomoto, K. 1987, *ApJ*, 322, 206

Nomoto, K., & Hashimoto, M. 1988, *Phys. Rep.*, 163, 13

Nomoto, K., Kobayashi, C., & Tomonaga, N. 2013, *ARA&A*, 51, 457

Oda, T., Hino, M., Muto, K., Takahara, M., & Sato, K 1994, *At. Data Nucl. Data Tables*, 56, 231

Richter, W. A., Mkhize, S., & Brown, B. A. 2008, *Phys. Rev. C*, 78, 064302

Slattery, W. L., Doolen, G. D., & DeWitt, H. E. 1982, *Phys. Rev. A*, 26, 2255

Suzuki, T., Honma, M., Mao, H., Otsuka, T. & Kajino, T 2011, *Phys. Rev. C*, 83, 044619

Suzuki, T., Toki, H., & Nomoto, K 2015, <http://w3p.phys.chs.nihon-u.ac.jp/~suzuki/data2/link.html>

Takahara, M., Hino, M., Oda, T., Muto, K., Wolters, A. A., Glaudemans, P. W. M., & Sato, K 1989, *Nucl. Phys. A*, 504, 167

Tilley, D. R., Cheves, C. M., Kelley, J. H., Raman, S., & Weller, H. R. 1998, *Nucl. Phys. A*, 636, 249

Toki, H., Suzuki, T., Nomoto, K., Jones, S., & Hirschi, R. 2013, *Phys. Rev. C*, 88, 015806

Wang, M., Audi, G., Wapstra, A. H., Kondev, F. G., MacCormik, M., Xu, X., & Pfeiffer, B. 2012, *Chinese Physics C*, 36, 1603

This 2-column preprint was prepared with the AAS L^AT_EX *harvard* v5.2.